Energy-Efficient Configuration of Frequency Resources in Multi-Cell MIMO-OFDM Networks[*]

Changyang She, Zhikun Xu, Chenyang Yang, Shengqian Han

Beihang University, Beijing, China
Email: shechangyang@sae.buaa.edu.cn, xuzhikun@ee.buaa.edu.cn,
cyyang@buaa.edu.cn and sqhan@ee.buaa.edu.cn

Chengjun Sun, Qi Wu

Beijing Samsung Telecom R & D Center, China
Email: {chengjun.sun, qi.wu}@samsung.com

Abstract—In this paper, we investigate the configuration of frequency resources from the perspective of maximizing the *energy efficiency* (EE) of downlink multi-cell multi-carrier multi-antenna systems. We first formulate an optimization problem of subcarrier assignment to minimize the total power consumption at the base stations under the constraints of *spectral efficiency* (SE) requirements from multiple users. Then we find its closed-form solution by analyzing different cases. Analytical and simulation results show that when the SE requirement is low, using non-overlapped frequency resources is more energy efficient than using overlapped frequency resources and the EE increases with the SE. To support high SE, more spatial resources should be configured but a trade-off between SE and EE appears. Serving cell-center users will provide higher EE, while when serving the cell-edge users maximizing the EE will lead to a minor loss of the SE.

I. INTRODUCTION

Energy efficiency (EE) is becoming one of the key design goal for future wireless communication networks [1–3]. In cellular systems, *multiple-input-multiple-output* (MIMO) and *orthogonal frequency division multiplexing* (OFDM) are popular techniques for providing high *spectral efficiency* (SE). However, how to improve their EE meanwhile ensure the required SE is not well-understood, especially when *inter-cell interference* (ICI) exists.

There have been some preliminary results on improving the EE of the multi-carrier multi-antenna systems. An overall discussion about developing energy-efficient MIMO radio was provided in [4], where various kinds of multi-antenna systems were considered. In [5], the EE of mobile stations (MSs) was maximized through uplink link adaptation under frequency-selective channels. In [6], both the configuration of active *radio frequency* (RF) chains and the frequency resource allocation among multiple MSs were studied for maximizing the EE of downlink MIMO-*orthogonal frequency division multiplexing multiple access* (OFDMA) systems. In [7], a distributed non-cooperative uplink OFDMA power allocation strategy was optimized and analyzed for multi-cell systems based on the game theory. Some interesting observations were obtained: the EE-oriented optimization is more beneficial for the interference
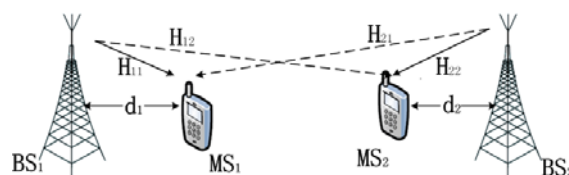

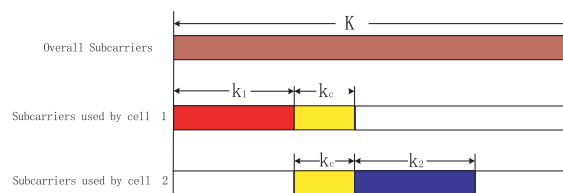Fig. 1. An example of the considered network

Fig. 2. Subcarrier assignment for two cells

limited scenarios and the EE is more sensitive to the power allocation than the SE.

In this paper, we study the configuration of frequency resource to maximum the EE of multi-cell downlink MIMO-OFDM systems, when the channel statistics are available at the *base stations* (BSs). Specifically, we will optimize the subcarrier allocation strategy to minimize the overall transmit and circuit power consumption at the BSs under the constraint of the average data rate requirements from multiple MSs, where ICI may exist to support high data rate. From the optimal solution we will analyze the impact of the spatial-frequency resources and user locations on the SE-EE relationship.

II. SYSTEM AND POWER CONSUMPTION MODEL

A. System Description

Consider a two-cell downlink MIMO-OFDM network, where one MS is located in each cell, as shown in Fig. 1. n_{t_1} and n_{t_2} antennas are respectively equipped at the two BSs, and n_r antennas are equipped at each MS. Overall K subcarriers are shared by the two cells.[*]

*Although we consider a two-cell system, the problem optimization and analysis results can be extended to multi-cell systems.
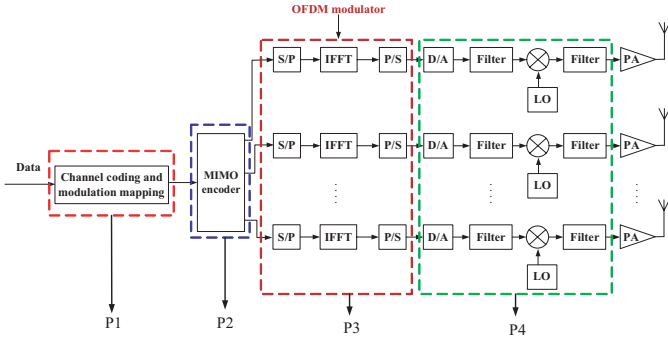
Fig. 3. Implementation structure of a MIMO-OFDM system

	Expression	Description
P1	$P_{c_1} R_i$	linearly increases with the data rate [8], R_i is the average data rate requirement of user i and P_{c_1} is a constant.
P2	$(\alpha n_t^2 + \beta n_t) P_{c_2}(k_i + k_c)$	linearly increases with the number of subcarriers used by BS_i. $(\alpha n_t^2 + \beta n_t) P_{c_2}$ is the power consumed by matrix operations on each subcarrier [9]. α, β, and P_{c_2} are constant.
P3	$n_t P_{c_3}(k_i + k_c)$	linearly increases with the number of used subcarriers and the number of transmit antennas [9]. P_{c_3} is a constant.
P4	$n_t P_{c_4}$	linearly increases with the number of transmit antennas [10]. P_{c_4} is a constant.

We assume that the MSs undergo frequency selective channels. The instantaneous *channel state information* (CSI) is unknown, but the channel distribution information is available at the BSs. Denote $\mathbf{H}_{i,j,m} \in \mathbb{C}^{n_r \times n_{t_i}}$ as the channel matrix from BS_i to MS_j on subcarrier m, whose elements are independent and identically Gaussian distributed with zero mean and variance $\mu_{i,j}$, where $\mu_{i,j}$ is the large-scale channel gain from BS_i to MS_j. The noise at each MS is assumed as additive white Gaussian with zero mean and variance σ_n^2.

We assume that different MSs can transmit their data both in the common and private frequency bands, as shown in Fig. 2. Denote k_c as the number of common subcarriers used by both cells, and k_1 and k_2 as the number of private subcarriers used by cell 1 and cell 2, respectively. Then we have

$$0 \le k_1 + k_c + k_2 \le K. \tag{1}$$

B. Power Consumption at the BSs

The total power consumed by the BSs consists of transmit power and circuit power. Denote ρ, P_{t_i} as the efficiency of the *power amplifier* (PA) at each antenna and the radiated power per antenna at each subcarrier of BS_i, respectively. Then the transmit power consumed by the PAs of BS_i can be expressed as $(k_i + k_c)\frac{n_{t_i} P_{t_i}}{\rho}$.

A typical implementation structure of a MIMO-OFDM system is shown in Fig. 3. The circuit power consumptions from different parts of the MIMO-OFDM system depend on different system parameters and are summarized in Table I. Based on the transmit power consumption and the circuit power consumption models, the total power consumed by the two BSs are

$$P_{tot} = (k_1 + k_c) \left[\frac{n_{t_1} P_{t_1}}{\rho} + (\alpha n_{t_1}^2 + \beta n_{t_1}) P_{c_2} + n_{t_1} P_{c_3} \right]$$
$$+ (k_c + k_2) \left[\frac{n_{t_2} P_{t_2}}{\rho} + (\alpha n_{t_2}^2 + \beta n_{t_2}) P_{c_2} + n_{t_2} P_{c_3} \right]$$
$$+ P_{c_1}(R_1 + R_2) + P_{c_4}(n_{t_1} + n_{t_2}) + 2P_{c_5} \tag{2}$$
$$= (k_1 + k_c)g(n_{t_1}) + (k_c + k_2)g(n_{t_2}) + f(n_{t_1}, n_{t_2}),$$

where P_{c_5} denotes the power consumption at each BS that is irrelative to the spatial and frequency resources, $g(n_{t_1}) \triangleq \frac{n_{t_1} P_{t_1}}{\rho} + (\alpha n_{t_1}^2 + \beta n_{t_1}) P_{c_2} + n_{t_1} P_{c_3}$ and $f(n_{t_1}, n_{t_2}) \triangleq P_{c_1}(R_1 + R_2) + P_{c_4}(n_{t_1} + n_{t_2}) + 2P_{c_5}$, and R_i denotes the

average data rate requirement of MS_i. Other parameters are described in Table I.

III. ENERGY EFFICIENCY OPTIMIZATION

In this section, we introduce the ergodic capacity of each MS, formulate an optimization problem that maximizes the downlink EE under the constraints on capacity requirements from both MSs, and finally provide a closed-form solution.

A. Ergodic Capacity for Each MS

From Fig. 2 we can see that the capacity for each MS is the sum of the capacities on the private subcarriers and the common subcarriers. The ergodic capacity of MS_i can be expressed as

$$C_i = \sum_{s=1}^{k_i} E_{i,s}^p + \sum_{t=1}^{k_c} E_{i,t}^c, \tag{3}$$

where $E_{i,s}^p$ and $E_{i,t}^c$ represent the ergodic capacities on the sth private subcarrier and the tth common subcarrier of MS_i, respectively.

Since only channel distribution information of each user is known at the BSs, from Shannon capacity formula [11] the ergodic capacity on the private subcarrier s of MS_i can be obtained as follows,

$$E_{i,s}^p = \Delta f \mathbb{E}_{\mathbf{H}_{i,i,s}} \{ \log_2 \det[\mathbf{I}_{n_r} + (\sigma_n^2 \mathbf{I}_{n_r})^{-1} P_{t_i} \mathbf{H}_{i,i,s} \mathbf{H}_{i,i,s}^H] \}$$
$$= \Delta f \mathbb{E}_{\widetilde{\mathbf{H}}_{i,i,s}} \left\{ \log_2 \det \left[\mathbf{I}_{n_r} + \frac{\mu_{i,i} P_{t_i}}{\sigma_n^2} \widetilde{\mathbf{H}}_{i,i,s} \widetilde{\mathbf{H}}_{i,i,s}^H \right] \right\}, \tag{4}$$

where $\mathbb{E}_{\mathbf{x}}\{\cdot\}$ is the expectation operation over $\mathbf{x}$, Δf is the subcarrier spacing, $\mathbf{I}_{n_r}$ denotes an $n_r \times n_r$ identity matrix, and $\widetilde{\mathbf{H}}_{i,i,s} \triangleq \frac{1}{\sqrt{\mu_{i,i}}} \mathbf{H}_{i,i,s}$. Because the elements of $\mathbf{H}_{i,i,s}$ are Gaussian distributed with zero mean and variance $\mu_{i,i}$, the elements of $\widetilde{\mathbf{H}}_{i,i,s}$ are normalized Gaussian random variables that are independent of the user index i and the subcarrier

index s. Consequently, $E_{i,s}^p$ is irrelevant to subcarrier index s. We denote it as E_i^p and (4) can be rewritten as

$$E_i^p = \Delta f \mathbb{E}_{\widetilde{\mathbf{H}}} \left\{ \log_2 \det \left[\mathbf{I}_{n_r} + \frac{\mu_{i,i} P_{t_i}}{\sigma_n^2} \widetilde{\mathbf{H}} \widetilde{\mathbf{H}}^H \right] \right\}, \quad (5)$$

where $\widetilde{\mathbf{H}} \triangleq \widetilde{\mathbf{H}}_{i,i,s}$ is an $n_r \times n_{t_i}$ matrix.

Similarly, the ergodic capacity on the common subcarrier t of MS_i can be expressed as

$$E_{i,t}^c = \Delta f \mathbb{E}_{\widetilde{\mathbf{H}}_1, \widetilde{\mathbf{H}}_2} \qquad (6)$$
$$\left\{ \log_2 \det \left[\mathbf{I}_{n_r} + \left(\sigma_n^2 \mathbf{I}_{n_r} + \mu_{ji} P_{t_j} \widetilde{\mathbf{H}}_1 \widetilde{\mathbf{H}}_1^H \right)^{-1} \mu_{ii} P_{t_i} \widetilde{\mathbf{H}}_2 \widetilde{\mathbf{H}}_2^H \right] \right\},$$

where $\widetilde{\mathbf{H}}_1 \triangleq \frac{1}{\sqrt{\mu_{j,i}}} \mathbf{H}_{j,i,t}$ and $\widetilde{\mathbf{H}}_2 \triangleq \frac{1}{\sqrt{\mu_{i,i}}} \mathbf{H}_{i,i,t}$ are both $n_r \times n_{t_i}$ matrices whose elements are normalized Gaussian random variables. We can see that the ergodic capacities on the common subcarrier are also irrelevant to t, hence we denote it as E_i^c.

Finally, the ergodic capacity for MS_i is

$$C_i = \sum_{s=1}^{k_i} E_i^p + \sum_{t=1}^{k_c} E_i^c = k_i E_i^p + k_c E_i^c. \qquad (7)$$

B. Subcarrier Assignment to Maximize the EE

To study the SE-EE relationship, we formulate a problem to maximize the EE of the downlink MIMO-OFDM under the constraints of average data rate requirement of each MS. When the average data rates of the MSs are given, maximizing the EE is equivalent to minimizing the total power consumption at both BSs. Considering (1), (2), and (7), the optimization problem to maximize the EE can be formulated as follows,

$$\min_{k_1, k_c, k_2} P_{tot} \qquad (8)$$

$$\text{s.t.} \quad k_1 E_1^p + k_c E_1^c = R_1, \qquad (8a)$$
$$k_2 E_2^p + k_c E_2^c = R_2, \qquad (8b)$$
$$0 \le k_1 + k_c + k_2 \le K, \qquad (8c)$$
$$k_1 \ge 0, k_c \ge 0, k_2 \ge 0. \qquad (8d)$$
$$k_1, k_c, \text{ and } k_2 \in \mathbb{Z} \qquad (8e)$$

where $\mathbb{Z}$ represents the set of integers and R_1 and R_2 denote the average data rate requirements of MS_1 and MS_2, respectively.

Because k_1, k_c, and k_2 are integer variables, it is very hard to find the optimal solution and we relax them to be continuous real variables. Without the constraint of (8e), it is easy to see that problem (8) is a linear programming with respect to k_1, k_c, and k_2.

From (8a) and (8b), we can obtain

$$k_1 = \frac{R_1 - k_c E_1^c}{E_1^p} \quad \text{and} \quad k_2 = \frac{R_2 - k_c E_2^c}{E_2^p}, \qquad (9)$$

respectively.

Substituting (9) into (2), (8c) and (8d), and ignoring constraint (8e), then problem (8) can be reformulated as

$$\min_{k_c} \left(\frac{R_1}{E_1^p} + \frac{E_1^p - E_1^c}{E_1^p} k_c \right) g(n_{t_1}) +$$
$$\left(\frac{R_2}{E_2^p} + \frac{E_2^p - E_2^c}{E_2^p} k_c \right) g(n_{t_2}) + f(n_{t_1}, n_{t_2}) \qquad (10)$$

$$\text{s.t.} \quad -\frac{R_1}{E_1^p} - \frac{R_2}{E_2^p} \le \left(1 - \frac{E_1^c}{E_1^p} - \frac{E_2^c}{E_2^p} \right) k_c \le K - \frac{R_1}{E_1^p} - \frac{R_2}{E_2^p}, \qquad (10a)$$

$$0 \le k_c \le \min \left\{ \frac{R_1}{E_1^c}, \frac{R_2}{E_2^c} \right\}. \qquad (10b)$$

In the following, we will find the closed-form solution of k_c. Comparing the ergodic capacity of each private subcarrier for MS_i shown in (5) with the ergodic capacity of each common subcarrier in (6), we can find that $E_i^p - E_i^c > 0$ because an ICI term, $\mu_{ji} P_{t_j} \widetilde{\mathbf{H}}_1 \widetilde{\mathbf{H}}_1^H$, exists in (6). Then the multiplicative coefficients of k_c in (10) are positive and the objective function, i.e., P_{tot}, is an increasing function of k_c. Therefore, the minimum value of the overall power consumption P_{tot} in problem (10) can be achieved when the value of k_c is the minimal value that satisfies the constraints (10a) and (10b). Such a k_c is the solution of the optimization problem.

To find the optimal value of k_c, we first find the intersection of (10a) and (10b). Because the sign of $1 - \frac{E_1^c}{E_1^p} - \frac{E_2^c}{E_2^p}$ determines the lower and upper bounds of the feasible set of k_c as shown in (10a), we analyze the following two cases.

C1. When $1 - \frac{E_1^c}{E_1^p} - \frac{E_2^c}{E_2^p} \ge 0$, the intersection of (10a) and (10b) depends on the sign of the right bound of (10a). When $K - \frac{R_1}{E_1^p} - \frac{R_2}{E_2^p} \ge 0$, we can see that $k_c = 0$ satisfies (10a). On the other hand, it is the left bound of (10b). Therefore, $k_c = 0$ is the minimum value that satisfies (10a) and (10b) and is the optimal solution of problem (10). When $K - \frac{R_1}{E_1^p} - \frac{R_2}{E_2^p} < 0$, it is readily shown that the intersection of (10a) and (10b) is an empty set and the outage occurs.

C2. When $1 - \frac{E_1^c}{E_1^p} - \frac{E_2^c}{E_2^p} < 0$, constraint (10a) becomes

$$\frac{\left(\frac{R_1}{E_1^p} + \frac{R_2}{E_2^p} - K \right)}{\left(\frac{E_2^c}{E_2^p} + \frac{E_1^c}{E_1^p} - 1 \right)} \le k_c \le \frac{\left(\frac{R_1}{E_1^p} + \frac{R_2}{E_2^p} \right)}{\left(\frac{E_2^c}{E_2^p} + \frac{E_1^c}{E_1^p} - 1 \right)}. \qquad (11)$$

(a) When the left bound of (11) is lower than the right bound of (10b), i.e.,

$$\frac{\left(\frac{R_1}{E_1^p} + \frac{R_2}{E_2^p} - K \right)}{\left(\frac{E_2^c}{E_2^p} + \frac{E_1^c}{E_1^p} - 1 \right)} \le \min \left\{ \frac{R_1}{E_1^c}, \frac{R_2}{E_2^c} \right\}, \qquad (12)$$

the constraints (10a) and (10b) have an intersection, and the minimal value of k_c can be expressed as

$$k_c^* = \max \left\{ 0, \frac{\left(\frac{R_1}{E_1^p} + \frac{R_2}{E_2^p} - K \right)}{\left(\frac{E_2^c}{E_2^p} + \frac{E_1^c}{E_1^p} - 1 \right)} \right\}. \qquad (13)$$

(b) Otherwise, the constraints (10a) and (10b) have no intersection, then an outage occurs.

The closed-form continuous solution of problem (10) is now obtained and is summarized in Table II.

We can conclude from the second and fourth lines of Table II that when the values of R_1 and R_2 satisfy $K - \frac{R_1}{E_1^p} - \frac{R_2}{E_2^p} \geq 0$, i.e., using the private subcarriers can satisfy the MSs' data rate requirements, the optimal value of k_c is 0. This imply that using subcarriers without overlap saves more energy than using the overlapped subcarriers.

When $K - \frac{R_1}{E_1^p} - \frac{R_2}{E_2^p} < 0$, i.e., using the private subcarriers cannot satisfy the MSs' data rate requirements, whether R_1 and R_2 can be achieved with the overall maximal K subcarriers depends on the sign of $1 - \frac{E_1^c}{E_1^p} - \frac{E_2^c}{E_2^p}$ and condition (12). The sign of $1 - \frac{E_1^c}{E_1^p} - \frac{E_2^c}{E_2^p}$ reflects the strength of ICI. When the ICI is small, the gap between E_i^c and E_i^p is small and the sign of this expression is negative. Otherwise, the sign is positive. Condition (12) actually provides an upper bound for R_1 and R_2. The results in the fifth line of Table II imply that R_1 and R_2 can be achieved by using common subcarriers only when the ICI is weak and the data rate is moderate such that it is not out of the upper bound provided by condition (12).

Based on the optimal continuous number of common subcarriers, k_c^*, in Table II, we can find the optimal continuous numbers of private subcarriers for MS1 and MS2, k_1^* and k_2^*, from (9). Then we can discretize the continuous solution by some existing methods [12].

IV. SIMULATION RESULTS

In this section, we will study the optimal subcarrier assignment strategies and the SE-EE relationship of the two-cell MIMO-OFDM system. The SE is defined as the overall data rate per unit bandwidth and the EE is defined as the data bits transmitted per unit energy.

We assume that both BSs have the same overall transmit power. The two MSs in the two cells are placed on the line between the two BSs and are away from their master BSs with the same distance d. We assume that the two MSs have the same SE requirement. The small-scale fading channel from each BS to each MS is subject to Gaussian distribution with zero mean and unit variance. All simulation results are obtained via 1000 channel realizations. The main system and channel parameters in the simulation are listed in Table III.

Figures. 4 and 5 show the optimal subcarrier assignment and the optimal EE under different SE requirements and different numbers of transmit antennas, respectively, where $d = 100$ m.

In Fig. 4, the left y-axis and the right y-axis respectively denote the optimal total number of used subcarriers, $k_1^* + k_c^* + k_2^*$, and the optimal number of common subcarriers, k_c^*. We can see that the optimal total number of used subcarriers increases with the SE linearly until it achieves the maximum value, K. It decreases with the number of transmit antennas, which implies a tradeoff between the frequency resource and spatial resource to achieve the same SE requirement. Note that the optimal numbers of the used subcarriers and the common subcarriers vary little for $n_t \geq 2$, but change rapidly for $n_t = 1$. This is because we consider $n_r = 2$ in the simulation.
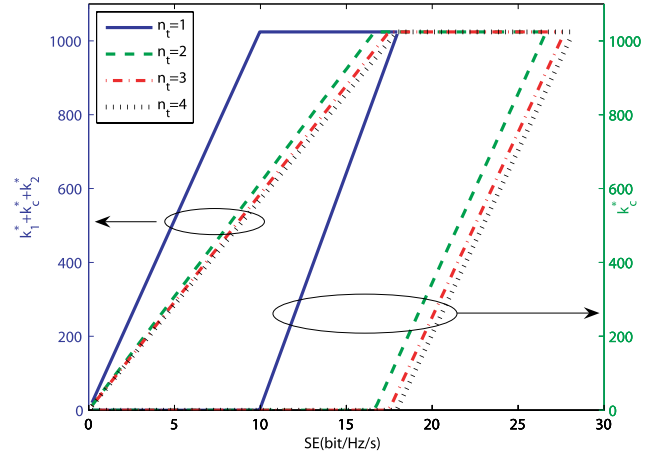

Fig. 4. Optimal subcarrier assignment strategies vs. the SE requirement when $d = 100$ m.
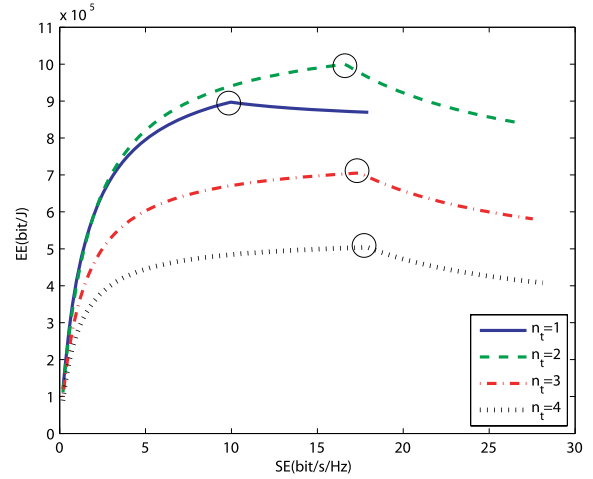

Fig. 5. SE-EE relationship with different values of n_t when $d = 100$ m.

When $n_t = 1$ the spatial multiplexing gain is one, therefore more subcarriers should be used to achieve high data rate. When $n_t \geq 2$ the spatial multiplexing gain is two, hence less subcarriers should be used to achieve the same data rate. We can also see that the optimal number of common subcarriers only appears when the all subcarriers are used. This means that subcarriers need to be reused only when using subcarriers without overlap cannot satisfy the SE requirements, which is consistent with the analysis in Section III.B.

In Fig. 5, we show the SE-EE relationship under various numbers of transmit antennas. Each curve can be divided into two parts by a transition point, which is marked with a circle. When the SE requirement is lower than the transition point, the optimal number of common subcarriers k_c^* is equal to zero, and the EE increases with the SE. Otherwise, $k_c^* > 0$. In this case, because ICI exists the EE decreases with the SE and a SE-EE tradeoff appears. We can see that $n_t = 2$ can achieve the highest EE, while $n_t = 4$ can achieve

$1 - \frac{E_1^c}{E_1^p} - \frac{E_2^c}{E_2^p}$	$K - \frac{R_1}{E_1^p} - \frac{R_2}{E_2^p}$	Condition (12)	Optimal value of k_c	Outage occurs?
≥ 0	≥ 0	——	$k_c^* = 0$	No
≥ 0	< 0	——	No solution	Yes
< 0	≥ 0	——	$k_c^* = 0$	No
< 0	< 0	Satisfied	$k_c^* = \dfrac{\left(\frac{R_1}{E_1^p} + \frac{R_2}{E_2^p} - K \right)}{\left(\frac{E_2^c}{E_2^p} + \frac{E_1^c}{E_1^p} - 1 \right)}$	No
< 0	< 0	Not satisfied	No solution	Yes

the highest SE, which comes from a coupled impact of the spatial multiplexing gain, spatial diversity gain, ICI and circuit power consumption. This is because two data streams can be transmitted at each subcarrier when $n_t \geq 2$, more spatial resources provide diversity gain and thus improves the SE a little, but also introduce larger circuit power consumption hence lead to a reduction of the EE.

Figure 6 shows the impact of the MS's location on the SE-EE relationship, where the optimized subcarrier assignment is applied. As expected, both the SE and EE reduce when the MSs move closer to the cell-edge for a given n_t, because the received SINR of each MS decreases. However, when the MSs approach the cell-edge, the SE loss reduces for achieving the maximal EE. For example, when $n_t = 1$ and $d = 100$ m, the maximum value of EE is 8.99×10^5 at the SE of 10 bps/Hz, and the maximum value of SE is 18 bps/Hz corresponding to an EE of 8.73×10^5. The SE loss is $(18 - 10)/18 = 44\%$ and the EE gain is $(8.99 - 8.73)/8.73 = 3\%$. When $n_t = 1$ and $d = 200$ m, the SE loss is $(10 - 6)/10 = 40\%$ and the EE gain is $(5.55 - 4.88)/4.88 = 13.7\%$. We can see that the SE loss is similar but the EE gain increases rapidly. When $n_t = 4$, we can observe that when the EE is maximized, there is no SE loss for the MSs located at $d = 200$ m and has about 35.7% SE loss for the MSs in $d = 100$ m. This observation implies that the EE oriented design is more beneficial for the cell-edge MSs. In other words, when ICI is severe for a give spatial-frequency resource configuration, maximizing the EE will lead to a minor SE loss.

V. CONCLUSIONS

In this paper, we have studied frequency resource configuration of a two-cell downlink MIMO-OFDM system to maximize the EE, when only channel statistical information is available at the BSs. We first formulated the optimization problem with respect to the numbers of common and private subcarriers, which minimized the overall transmit and circuit power consumed at the BSs under the constraints of the average data rate requirements from the MSs. We then found the close-form solution. Analysis and simulation results revealed an intricate impact of the multiplexing gain, diversity gain and inter-cell interference contributed by the spatial resources, the high capacity contributed by increasing the frequency resources, and the circuit power consumption on the SE-

TABLE III
LIST OF SIMULATION PARAMETERS

| Subcarrier spacing, Δf	15 kHz
Number of antennas at the BSs, $n_t = n_{t_1} = n_{t_2}$	1, 2, 3, 4
Overall transmit power of the BSs, $P_{t_1}^{tot} = P_{t_2}^{tot}$	46 dBm
Number of antennas at each MS, n_r	2
Radius of each cell, R	250 m
SNR at the edge of each cell	10 dB
Minimum distance from BS to MS	35 m
Path loss	$35 + 38 \log_{10} d$ (dB)
Efficiency of power amplifier, ρ	38%
Total number of subcarriers, K	1024
P_{c1}	1.95×10^{-4} mW
αP_{c2}	20 mW
$\beta P_{c2} + P_{c3}$	20 mW
P_{c4}	1000 mW
P_{c5}	10000 mW
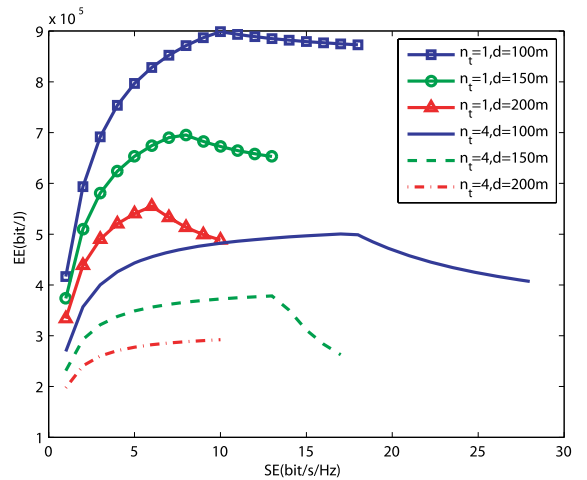
Fig. 6. SE-EE relationship with different values of d.

EE relationship. In the low SE region, increasing the non-overlapped frequency resources is more beneficial to provide high EE, and the EE increases with the SE. In the high SE region, more spatial resources should be applied but the EE will reduce. For the cell-edge users, maximizing the EE will lead to minor loss of SE. Although we considered a two-cell system, the optimization problem, the solution and the analysis results can be easily extended into general multi-cell systems.

REFERENCES

[1] G. Y. Li, Z. Xu, C. Xiong, C. Yang, S. Zhang, Y. Chen, and S. Xu, "Energy-efficient wireless communications: tutorial, survey, and open issues," *IEEE Wireless Commun. Mag.*, vol. 18, no. 6, pp. 28–35, Dec. 2011.

[2] L. M. Correia, D. Zeller, O. Blume, D. Ferling, Y. Jading, I. Godor, G. Auer, and L. V. der Perre, "Challenges and enabling technologies for energy aware mobile radio networks," *IEEE Communications Mag.*, vol. 48, no. 11, pp. 66–72, Nov. 2010.

[3] Y. Chen, S. Zhang, S. Xu, and G. Y. Li, "Fundamental tradeoffs on green wireless networks," *IEEE Commun. Mag.*, vol. 49, no. 6, pp. 30–37, Jun. 2011.

[4] R. Eickhoff, R. Kraemer, I. Santamaria, and L. Gonzalez, "Developing energy-efficient MIMO radios," *IEEE Vehicular Technology Mag.*, pp. 34–41, Mar. 2009.

[5] G. Miao, N. Himayat, and G. Y. Li, "Energy-efficient link adaptation in frequency-selective channels," *IEEE Trans. Commun.*, vol. 58, no. 2, pp. 545–554, Feb. 2010.

[6] Z. Xu, C. Yang, G. Li, S. Zhang, Y. Chen, and S. Xu, "Energy-efficient configuration of spatial and frequency resources in MIMO-OFDMA systems," *to appear in Proc. IEEE ICC*, Jun. 2012.

[7] G. Miao, N. Himayat, and G. Y. Li, "Distributed interference-aware energy-efficient power optimization," *IEEE Trans. Commun.*, vol. 58, no. 2, pp. 545–554, Feb. 2010.

[8] C. Isheden and G. P. Fettweis, "Energy-efficient multi-carrier link adaptation with sum rate-dependent circuit power," in *IEEE Proc. GlobeCom*, Dec. 2010.

[9] H. S. Kim and B. Daneshrad, "Energy-constrained link adaptation for MIMO OFDM wireless communication systems," *IEEE Trans. Wireless Commun.*, vol. 9, no. 9, pp. 2820–2832, Sep. 2010.

[10] S. Cui, A. J. Goldsmith, and A. Bahai, "Energy-efficiency of MIMO and cooperative MIMO techniques in sensor networks," *IEEE J. Select. Areas Commun.*, vol. 22, no. 6, pp. 1089–1098, Aug. 2004.

[11] D. Tse and P. Viswanath, *Fundamentals of wireless communication*. Cambridge Univ. Press, 2005.

[12] Z. Xu, C. Yang, G. Li, S. Zhang, Y. Chen, and S. Xu, "Energy-efficient MIMO-OFDMA systems based on switching off RF chains," in *Proc. IEEE VTC Fall*, Sep. 2011.